Innovare Academic Sciences

International Journal of Pharmacy and Pharmaceutical Sciences

ISSN- 0975-1491 Vol 6, Issue 7, 2014

Original Article

MUTAGENICITY PREDICTION FOR NITROAROMATIC COMPOUNDS USING QSTR MODELING

NILESH TAWARI, ARUNDHATI LELE, MIHIR KHAMBETE, MARIAM DEGANI*

Department of Pharmaceutical Sciences and Technology, Institute of Chemical Technology, Matunga (E), Mumbai 400019, India.
Email: msdegani@gmail.com

Received: 19 June 2014 Revised and Accepted: 20 Jul 2014

ABSTRACT

Objective: Nitroaromatic compounds are important industrial chemicals widely used in the synthesis of many diverse products including drugs, dyes, polymers, pesticides and explosives. However, the mutagenicity associated with nitroaromatic compounds is a toxicological feature which poses great concern. On the other hand, there are successful examples of non-mutagenic nitroaromatic molecules; indicating that safer nitroaromatic compounds can be developed. In this light the aim of the present work was to predict the mutagenicity of nitroaromatic compounds using an atom based QSTR model.

Methods: An atom based QSTR model was developed using PHASE. In addition, molecules were studied by complete geometry optimization using DFT at B3LYP/3-21G* level of theory.

Results: An atom based QSTR model was generated for prediction of mutagenicity of the compounds.

Conclusion: The visualization of different properties highlighted key inferences. These include the likelihood of mutagenicity for the molecules with more fused planar hydrophobic rings having hydrogen bond acceptor and electron donating substitutions. Also, all highly mutagenic compounds have two or more negative potential regions. Specific electronic properties such as HOMO and LUMO indicate that most of the mutagenic molecules are very reactive in nature. The results of this study would be useful as a predictive tool to screen out mutagenic nitroarenes and design safer non-mutagenic nitro compounds.

Keywords: Nitroaromatic, Mutagenicity, Molecular electrostatic profile (MESP), lowest unoccupied molecular orbital (LUMO), Quantitative Structure Toxicity Relationship (QSTR).

INTRODUCTION

Nitroaromatic compounds are widely used in a variety of chemical industries as intermediates, and are amongst major environmental pollutants released from automobile exhausts and industrial areas. These industry effluents have proved to be potent mutagens or carcinogens [1]. Also, many drugs in the market (e.g. tolcapone, nimesulide, nilutamide, flutamide, nitrofurantoin) and some under clinical studies (e.g. PA-824 and OPC-67683) have nitro substituents [2-5]. However the toxicities of such nitroaromatic compounds limit their development and use. In the past few decades, the pharmacological and toxicological properties of nitroarenes have been extensively studied [6]. Nitroarenes possess genotoxic properties as they can form various electrophilic intermediates and adducts with DNA, tissue proteins, blood proteins albumin and hemoglobin [7]. Nitroaromatic compounds are linked to mutagenicity and carcinogenicity [8,9]. Analysis of 224 chemicals performed by Zeiger et al. revealed that all nitro carcinogens were mutagenic in behavior [10]. Recently, Benigni et al. reviewed theoretical models on the relationship between chemical structure and the molecular mechanisms of toxic activity of nitroaromatic compounds [11].

There is an increasing public concern over the toxicity of chemicals, including nitroaromatics, which has generated great interest in the field of predictive toxicology. The goal of predictive toxicology is to develop models that can predict the toxicities of the compounds on the basis of prior knowledge of the structure of a chemical compound. For many years, various QSAR techniques have been efficiently used to develop relationship between the structure of a molecule and the toxicity mechanisms, for a variety of reactive chemical classes [12]. One such method to judge the toxicity of molecules is to develop quantitative structure toxicity relationship (QSTR) models for toxic end-points such as mutagenicity. The QSTR modeling is encouraging for screening new compounds and helps to overcome the time and cost associated with the animal studies. QSTR modeling for toxicity has several difficulties, including diversity of molecules, multiple mechanisms involved in toxicological effects and different methods used for determination of toxicity. To correlate the mutagenicity with free energy change the revertants data from Ames test of mutagenicity is used for building QSTR models of mutagenic compounds [13-17]. Ames test (*Salmonella typhimurium* his reversion assay) is a simple and economical method for finding out mutagenic potential of the compounds. It is performed on different strains of *S. typhimurium* depending on the mechanism and metabolic activation of different classes of carcinogens [18-21]. *S. typhimurium* TA98 strain undergoes mutations in presence of nitro compounds; hence several attempts have been made for *in-silico* prediction of mutagenicity on the data generated from TA98 strain [22,23].

Very little success has been achieved in modeling of mechanistically complex side effects such as hepatotoxicity, carcinogenicity and reproductive effects. However, there are reported QSTR models for predicting toxicity for individual chemical classes such as quinolones [24-26], nitroarenes [1,27], aromatic amines [28,29], triazines [30], polycyclic aromatic hydrocarbons [31,32] and lactones [33,34] which cause toxicity by similar mechanisms.

In the present work, the individual atom based QASR module of Pharmacophore Alignment and Scoring Engine (PHASE) in Schrödinger suite, was used to develop an atom based 3DQSAR model for predicting the mutagenicity of nitroaromatic compounds. In addition, several quantum chemical descriptors including the lowest unoccupied molecular orbital (LUMO), highest occupied molecular orbital (HOMO), locations of three dimensional molecular electrostatic potentials were calculated, which are expected to provide an insight into mechanistic details of mutagenicity. The models thus developed can be used for mutagenicity prediction of various nitroaromatic compounds.

MATERIALS AND METHODS

A set of 197 nitroaromatic compounds (Table 1) with diverse structural variation ranging from a single benzene ring to coronene which consists of six fused benzene rings was collected from the publications of Goldring et al. [35], Rosenkranz et al. [36], Zielinska

et al. [37] and was used to derive QSTR model. The mutagenicity of the above compounds has been reported on *S. typhimurium* TA98 strain. To minimize the experimental errors, due to variation in assay techniques or laboratory conditions, the average of log revertants/nmol values of mutagenicity data was used as the dependent variable in QSTR modeling. Compounds were divided into a training set (148 compounds) and a test set (49 compounds) using randomization as well as chemical and biological diversity (Table 1a and 1b). This dataset has been used for QSTR modeling by Hansch et al. [1] and more recently by Nair et al. [27].

QSTR model generation

The 3D-QSAR model generation was carried out using PHASE, [38] version 3.0, Schrödinger, LLC, New York, NY, 2008 installed on Intel Pentium 4 computer. A unique low-energy 3D structure was generated for each ligand with the help of Ligprep, where appropriate hydrogens were added to all structures and were subsequently subjected to energy minimization using the OPLS-2005 force field with a constant dielectric of 1.0. The structures were imported to "individual QSAR model" panel in the PHASE. The dataset was divided into a training set of one hundred and forty eight molecules and a test set of forty nine molecules, randomly, incorporating biological and chemical diversity. A rectangular grid with spacing of 1.0Å was defined to encompass the space occupied by the aligned training set molecules. Based on the occupation of a cube by a ligand atom of training set molecules, total number of volume bits were assigned to a given cube. Thus, molecules were represented by a string of zeros and ones, according to the cubes it occupies and the different types of atoms/sites that reside in those cubes. QSAR models were generated by applying partial least squares (PLS) regression to this pool of binary-valued independent variables and using mutagenicity as dependent variable. Models were generated for one to ten PLS factors. Each of these models was validated using a test set of forty nine molecules which were not considered during model generation.

Density functional theory calculations

All compounds were used for density functional theory (DFT) calculations using Jaguar, version 7.5, Schrödinger, LLC, New York, NY, 2008 installed on Intel Pentium 4 computer. Complete geometry optimization was carried out using hybrid density functional theory with Becke's three-parameter exchange potential and the Lee-Yang-Parr correlation functional (B3LYP) [39-41], using basis set 3-21G* level [42-44]. To simulate physiological conditions, energy calculations were performed in aqueous environment using the Poisson-Boltzmann solver. In the present work, MESP V(r) at a point r due to a molecular system with nuclear charges {ZA} located at {RA} and the electron density ρ(r) were derived using following equation.

$$V(r) = \sum_{A=1}^{N} \frac{Z_A}{|r - R_A|} - \int \frac{\rho(r')d^3r'}{|r - r'|} \quad \text{..... (1)}$$

In Eq. (1) N denotes the total number of nuclei in the molecule and the two terms refer to the bare nuclear potential and the electronic contributions, respectively. The balance of these two terms brings about the effective localization of electron-rich regions in the molecular system. Molecular electrostatic properties including 3D-molecular electrostatic potentials (MESP), dipole moment, LUMO, HOMO and aqueous solvation energy were computed using Jaguar. MESP maps and their electrostatic potential energy isopotential profiles were generated using Maestro 8.0.

The MESP isoenergy contours were generated at -30.0 kcal/mol. The electrostatic potentials were sampled over the entire accessible surface of a molecule (corresponding roughly to van der Waals contact surface) and over the space extending beyond the molecular surface, providing a measure of charge distribution from the point of view of an approaching reagent.

The regions of positive electrostatic potential indicate excess positive charge, i.e., repulsion for the positively charged test probe; while regions of negative potential indicate areas of excess negative charge, i.e., attraction of the positively charged test probe. Three-dimensional isosurfaces of the MESPs at the van der Waals contact surface represent electrostatic potentials superimposed onto a surface of constant electron density (0.01 e/au$_3$).

These color coded isosurface values provide an indication of overall molecular size and of the location of negative or positive electrostatic potentials. The most negative electrostatic potential is colored deepest red (the most nucleophilic site) and the most positive electrostatic potential is colored deepest blue (the most electrophilic site). The intermediate shades (orange, yellow, green) indicate intermediate ranges of reactivity.

Table 1a:The actual and predicted mutagenicity values training set of compounds with their logP (taken from reference 30) and calculated HOMO and LUMO energy at B3LYP/3-21G* level of theory.

S. No.	Compound Name	LogP[30]	Activity	PHASE predicted activity	HOMO (eV)	LUMO (eV)
1	1,8-dinitropyrene	4.44	5.39	4.02	-0.24	-0.13
2	1,6-dinitropyrene	4.44	5.06	4.00	-0.24	-0.13
3	3,9-dinitrofluoranthene	4.44	5.02	5.02	-0.25	-0.12
4	1,3,6-trinitropyrene	4.18	4.99	5.71	-0.25	-0.14
5	1,3,6,8-tetranitropyrene	3.92	4.99	4.96	-0.26	-0.16
6	2,7-dinitrophenazine	2.29	4.34	4.02	-0.26	-0.14
7	5,8-dinitrobenzo[ghi] perylene	6.07	4.33	4.24	-0.22	-0.13
8	2,7-dinitro-4,5-dihydro pyrene	4.73	4.25	4.30	-0.24	-0.12
9	1-nitro-3-acetoxypyrene	4.42	4.22	4.30	-0.22	-0.11
10	2-nitrotriphenylene	5.41	4.09	1.90	-0.24	-0.11
11	8-nitrofluoranthene	4.69	4.05	2.44	-0.24	-0.11
12	2,4-dinitrofluoranthene	4.44	3.78	3.26	-0.25	-0.13
13	3,4-dinitrofluoranthene	4.44	3.62	3.89	-0.25	-0.12
14	5,10-dinitrobenzo[ghi] perylene	6.07	3.60	3.18	-0.23	-0.13
15	2,7-dinitro-4,5,9,10-tetrahydropyrene	5.02	3.50	3.38	-0.24	-0.12
16	2,3,5-trinitrofluoranthene	4.18	3.44	3.22	-0.25	-0.14
17	2,4,7-trinitro-9-fluorenone	2.42	3.41	3.67	-0.28	-0.14
18	2-nitropyrene	4.69	3.35	2.35	-0.22	-0.10
19	2-nitro-4,5-dihydropyrene	4.99	3.27	3.33	-0.23	-0.10
20	2,7-dinitrofluorene	3.35	3.22	3.05	-0.25	-0.12
21	2,7-dinitro-9-fluorenone	2.84	3.19	2.43	-0.27	-0.13

RESULTS AND DISCUSSION

To build a QSTR model for the prediction of mutagenicity of nitroaromatic compounds, atom-based QSAR model studies were carried out using "individual QSAR model" option in PHASE using PLS method. The summary of statistical data for models generated using 1 to 10 PLS factors is listed in Table 2. Considering the overall performance of various QSAR models with respect to different statistical parameters such as r2, Q2, Pearson-R, SD, RMSE and F-value used for the selection of best QSAR model, the model associated with 5 PLS factors, showed excellent internal and external predictive power, hence this model was used for further studies. Figure 1 shows the linearity trend in the graphs of actual vs. predicted activity for training and test set molecules.The actual and predicted values of mutagenicity are listed in Table 1a and 1b, for training and test set respectively.

Table 1a:The actual and predicted mutagenicity values training set of compounds with their logP (taken from reference 30) and calculated HOMO and LUMO energy at B3LYP/3-21G* level of theory.

S. No.	Compound Name	LogP[30]	Activity	PHASE predicted activity	HOMO (eV)	LUMO (eV)
22	1,2,5-trinitrofluoranthene	4.18	3.16	3.79	-0.25	-0.13
23	2-chloro-7-nitrofluorene	4.68	3.11	2.82	-0.24	-0.10
24	1,2-dinitrofluoranthene	4.44	3.11	3.26	-0.24	-0.12
25	trans-7,8-dihydro-3-nitrobenzo[a] pyrene-7,8-diol	3.01	3.08	2.66	-0.22	-0.11
26	2-nitrofluoranthene	4.69	3.01	2.94	-0.24	-0.11
27	2-iodo-7-nitrofluorene	5.09	2.97	3.13	-0.23	-0.10
28	3-nitrobenzo[e]pyrene	5.87	2.95	2.42	-0.23	-0.11
29	2,4,5,7-tetranitro-9-fluorenone	2.40	2.93	2.32	-0.29	-0.16
30	3,4,3',4'-tetranitrobiphenyl	3.00	2.85	2.36	-0.28	-0.14
31	3-nitro-benzo[a]pyrene	5.87	2.82	2.79	-0.21	-0.11
32	2-[(trifluoroacetyl)amino]-7-nitrofluorene	4.23	2.81	2.00	-0.23	-0.10
33	trans-9,10-dihydro-3-nitrobenzo[a] pyrene-9,10-diol	3.01	2.80	2.56	-0.22	-0.11
34	2-methoxy-7-nitrofluorene	3.95	2.79	3.13	-0.22	-0.10
35	1-nitropyrene	4.69	2.78	2.94	-0.22	-0.11
36	3-nitrobenzo[k]fluor anthene	5.87	2.76	2.70	-0.22	-0.11
37	2-fluoro-7-nitrofluorene	4.11	2.68	3.36	-0.24	-0.10
38	2,4,2',4'-tetranitrobiphenyl	3.00	2.66	2.57	-0.29	-0.13
39	1-nitrobenzo[a]pyrene	5.87	2.63	2.00	-0.21	-0.11
40	2,3-dinitrofluoranthene	4.44	2.62	3.44	-0.24	-0.13
41	3,4,4'-trinitrobiphenyl	3.26	2.60	3.10	-0.27	-0.13

Table 1a: The actual and predicted mutagenicity values training set of compounds with their logP (taken from reference 30) and calculated HOMO and LUMO energy at B3LYP/3-21G* level of theory.

S. No.	Compound Name	LogP[30]	Activity	PHASE predicted activity	HOMO (eV)	LUMO (eV)
42	1-methyl-2-nitrobenz imidazole	1.58	2.54	1.03	-0.25	-0.11
43	N'(5nitro2furfuryliden) 5nitro2furanacrylohydrazide	2.79	2.45	2.72	-0.24	-0.12
44	1,3-dinitro-9,10,11,12-tetrahydrobenzo[e]pyrene	6.01	2.41	3.57	-0.23	-0.12
45	1,6-dinitro-9,10,11,12-tetrahydrobenzo[e]pyrene	6.01	2.41	2.65	-0.23	-0.13
46	2,5-dinitrofluoranthene	4.44	2.32	2.12	-0.25	-0.12
47	2-hydroxy-1-nitrofluor Anthene	4.66	2.26	1.85	-0.23	-0.11
48	9-nitrophenanthrene	4.23	2.25	0.73	-0.24	-0.11
49	3-nitro-9-fluorenone	3.06	2.13	2.05	-0.25	-0.12
50	2-nitrophenanthrene	4.23	2.11	2.32	-0.23	-0.11
51	2-nitrophenazine	2.52	2.06	2.47	-0.25	-0.12
52	1,7-dinitrophenazine	2.29	2.02	1.64	-0.26	-0.13
53	1,6-dinitrobenzo[e]pyrene	5.61	1.99	2.71	-0.24	-0.12
54	3,4,3'-trinitrobiphenyl	3.26	1.92	2.02	-0.27	-0.13
55	10-hydroxy-1-nitropyrene	4.34	1.89	1.92	-0.21	-0.08
56	7-nitrofluoranthene	4.69	1.87	2.01	-0.24	-0.11
57	2-acetoxy-7-nitrofluorene	3.46	1.86	2.08	-0.23	-0.10
58	2-nitrodibenzo-1,4-dioxin	4.73	1.79	2.34	-0.22	-0.10
59	1-nitroacenaphthylene	2.72	1.77	1.96	-0.25	-0.12
60	3-nitroacenaphthylene	3.36	1.77	1.32	-0.24	-0.12
61	7-nitro-2,3-dichlorodibenzo -1,4-dioxin	6.24	1.73	1.29	-0.23	-0.11
62	2-nitrodibenzofuran	3.83	1.64	1.36	-0.25	-0.10

Table 1a:The actual and predicted mutagenicity values training set of compounds with their logP (taken from reference 30) and calculated HOMO and LUMO energy at B3LYP/3-21G* level of theory.

S. No.	Compound Name	LogP[30]	Activity	PHASE predicted activity	HOMO (eV)	LUMO (eV)
63	1-nitrobenzo[e]pyrene	5.87	1.59	2.26	-0.22	-0.11
64	2-nitro-4,5,9,10-tetrahydropyrene	5.28	1.58	1.07	-0.23	-0.10
65	2-amino-7-nitrofluorene	3.06	1.56	1.45	-0.19	-0.10
66	2,3,5-trinitronaphthalene	2.55	1.51	1.62	-0.27	-0.13
67	2-nitrofluorene	3.37	1.43	0.49	-0.24	-0.10
68	6-hydroxy-1-nitropyrene	4.19	1.34	2.84	-0.21	-0.11
69	1,9-dinitrophenazine	2.29	1.26	1.40	-0.24	-0.13
70	2,4-dinitro-1-fluorobenzene	1.49	1.20	0.88	-0.30	-0.12
71	4,4'-dinitrobiphenyl	3.52	1.17	0.40	-0.26	-0.11
72	3-nitroacenaphthene	3.81	1.00	1.37	-0.23	-0.10
73	5-nitrobenz[k]acephen anthrylene	5.07	0.92	1.38	-0.22	-0.12
74	1,8-dinitronaphthalene	2.52	0.90	2.36	-0.26	-0.11
75	1-nitro-7,8,9,10-tetrahydro benzo[a]pyrene	6.57	0.90	0.45	-0.22	-0.11
76	1-nitrophenazine	2.52	0.87	-0.12	-0.25	-0.12
77	2-nitrobenz[j]aceanthrylene	5.07	0.86	1.07	-0.23	-0.12
78	4-nitrocyclopenta[cd]pyrene	4.35	0.77	1.27	-0.23	-0.12
79	1-nitro-9,10,11,12-tetrahydrobenzo[e]pyrene	6.26	0.70	1.16	-0.22	-0.11
80	4-nitrobenz[k]acephen anthrylene	5.07	0.67	1.35	-0.22	-0.12
81	6-nitroindazole	2.06	0.66	-0.07	-0.24	-0.11
82	2,4,4'-trinitrobiphenyl	3.26	0.66	-0.29	-0.27	-0.12
83	4-nitro-o-phenylenediamine	0.88	0.63	-0.52	-0.19	-0.08
84	5-nitroacenaphthene	3.85	0.58	0.63	-0.23	-0.10

Table 1a: The actual and predicted mutagenicity values training set of compounds with their logP (taken from reference 30) and calculated HOMO and LUMO energy at B3LYP/3-21G* level of theory.

S. No.	Compound Name	LogP[30]	Activity	PHASE predicted activity	HOMO (eV)	LUMO (eV)
85	1,5-dinitronaphtalene	2.58	0.52	-0.09	-0.26	-0.12
86	1-nitrocoronene	6.79	0.45	1.13	-0.22	-0.11
87	1,3,8-trinitronaphthalene	2.30	0.35	0.06	-0.27	-0.13
88	1-chloro-2,4-dinitrobenzene	2.17	0.30	0.63	-0.29	-0.12
89	3-nitro-7,8,9,10-tetrahydro benzo[a]pyrene	6.57	0.30	1.46	-0.22	-0.11
90	3-amino-4'-nitrobiphenyl	2.68	0.25	-0.38	-0.20	-0.10
91	4,3'-dinitrobiphenyl	3.52	0.23	1.23	-0.26	-0.11
92	4-amino-4'-nitrobiphenyl	2.68	0.19	0.09	-0.20	-0.10
93	1,4-dinitrobenzene	1.46	0.15	-0.51	-0.29	-0.13
94	5-nitroindene	2.74	0.08	-0.22	-0.24	-0.10
95	6-nitrobenz[e]aceanthrylene	5.07	0.04	-0.14	-0.22	-0.12
96	1,3-dinitrobenzene	1.49	0.03	-0.02	-0.30	-0.12
97	2,4,3'-trinitrobiphenyl	3.26	0.03	-0.20	-0.27	-0.12
98	3-methyl-2-nitronaphthalene	3.43	0.00	-0.11	-0.23	-0.10
99	1,3-dinitronaphthalene	2.83	-0.05	0.13	-0.26	-0.12
100	2,4-dinitrophenylhydrazine	1.46	-0.07	-0.63	-0.23	-0.11
101	2,4,2',6'-tetranitrobiphenyl	3.00	-0.07	0.48	-0.28	-0.13
102	3-methyl-4-nitrobiphenyl	3.99	-0.10	-0.45	-0.25	-0.10
103	2-nitrochrysene	5.41	-0.22	-0.18	-0.22	-0.11
104	5-nitrochrysene	5.41	-0.22	0.24	-0.22	-0.11
105	4-fluoronitrobenzene	1.80	-0.23	0.45	-0.27	-0.10
106	2'-methyl-4-nitrobiphenyl	4.27	-0.23	-0.60	-0.25	-0.10

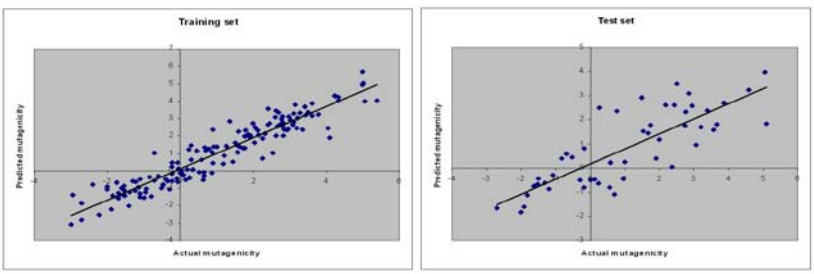

Fig.1: Scatter plots for the predicted and experimental mutagenicity values for the QSTR model applied to the training set and the test set; $r^2 = 0.90$, $Q^2 = 0.64$ and Pearson-R = 0.81.

Table 1a:The actual and predicted mutagenicity values training set of compounds with their logP (taken from reference 30) and calculated HOMO and LUMO energy at B3LYP/3-21G* level of theory.

S. No.	Compound Name	LogP[30]	Activity	PHASE predicted activity	HOMO (eV)	LUMO (eV)
107	4-nitrobiphenyl	3.77	-0.30	-1.08	-0.25	-0.10
108	3-nitro-1,2,4,7,8-pentachloro dibenzo-1,4-dioxin	7.84	-0.33	-0.60	-0.24	-0.12
109	2-methyl-6-nitroindazole	1.77	-0.41	-0.47	-0.23	-0.10
110	6-nitroindoline	1.92	-0.48	-0.78	-0.20	-0.09
111	2-methyl-5-nitrobenz imidazole	1.94	-0.51	-1.00	-0.25	-0.10
112	1-nitronaphthalene	3.19	-0.61	-0.31	-0.24	-0.11
113	3-nitrocarbazole	3.51	-0.70	1.04	-0.24	-0.10
114	1-methyl-2-nitronaphthalene	3.43	-0.70	-0.55	-0.24	-0.10
115	2,5-difluoronitrobenzene	1.89	-0.79	-1.49	-0.27	-0.11
116	3,2'-dimethyl-4-nitro biphenyl	4.49	-0.84	-0.34	-0.25	-0.10
117	5-nitroisatin	0.47	-0.94	-1.02	-0.26	-0.12
118	5-nitroquinoline	1.86	-0.96	-1.22	-0.26	-0.11
119	1-methyl-7-nitroindazole	1.77	-1.00	-1.54	-0.24	-0.10
120	2-methyl-5-nitroindazole	1.77	-1.10	-0.48	-0.23	-0.10
121	1-methyl-6-nitroindazole	1.77	-1.10	-1.31	-0.24	-0.11
122	2-nitro-p-phenylenediamine	0.53	-1.11	-1.49	-0.18	-0.08
123	4-nitrochalcone	2.83	-1.15	-0.94	-0.24	-0.12
124	6-methoxy-8-nitroquinoline	1.87	-1.21	-0.65	-0.24	-0.11
125	8-nitroquinoline	1.44	-1.24	-1.15	-0.25	-0.10
126	4-nitrostyrene	2.61	-1.30	-0.61	-0.25	-0.10
127	2-nitro-1,3,7,8-tetrachloro dibenzo-1,4-dioxin	7.13	-1.40	-1.24	-0.23	-0.11

Table 1a:The actual and predicted mutagenicity values training set of compounds with their logP (taken from reference 30) and calculated HOMO and LUMO energy at B3LYP/3-21G* level of theory.

S. No.	Compound Name	LogP[30]	Activity	PHASE predicted activity	HOMO (eV)	LUMO (eV)
128	4,4'-dinitrochalcone	2.73	-1.42	-2.03	-0.26	-0.12
129	2-amino-3'-nitrobiphenyl	2.68	-1.52	-1.44	-0.20	-0.10
130	4-nitroacetophenone	1.53	-1.54	-0.88	-0.27	-0.11
131	2,5-dichloronitrobenzene	2.90	-1.54	-1.42	-0.27	-0.11
132	5-nitroisoquinoline	1.65	-1.55	-1.11	-0.26	-0.11
133	metronidazole	-0.02	-1.61	-1.01	-0.26	-0.10
134	1-nitro-2,4-difluorobenzene	1.89	-1.66	-1.36	-0.28	-0.10
135	3-amino-3'-nitrobiphenyl	2.68	-1.70	-1.26	-0.20	-0.10
136	2-amino-4'-nitrobiphenyl	2.68	-1.70	-1.60	-0.20	-0.10
137	2-chloronitrobenzene	2.24	-1.72	-1.53	-0.27	-0.11
138	2,4-dinitroaniline	1.84	-1.74	-0.67	-0.24	-0.11
139	3,4-dinitro-1-fluorobenzene	1.89	-1.84	-1.42	-0.28	-0.13
140	2,4-dinitroanisole	1.72	-1.89	-2.21	-0.26	-0.11
141	4-nitrocarbazole	3.51	-2.00	-1.07	-0.24	-0.13
142	3-amino-2'-nitrobiphenyl	2.68	-2.00	-0.90	-0.19	-0.10
143	2-nitrophenetole	2.35	-2.22	-2.54	-0.24	-0.09
144	2-amino-5-nitrophenol	1.36	-2.40	-0.78	-0.20	-0.08
145	2-nitroanisole	1.73	-2.70	-2.80	-0.24	-0.09
146	8-nitroquinaldine	1.99	-2.70	-1.85	-0.25	-0.10
147	1,2,3-trichloro-4- nitrobenzene	3.61	-2.94	-1.38	-0.28	-0.12
148	2-nitro-m-phenylenediamine	0.87	-3.00	-3.07	-0.19	-0.08

Table 1b:The actual and predicted mutagenicity values test set of compounds with their logP (taken from reference 30) and calculated salvation, LUMO energy at B3LYP/3-21G* level of theory.

S. No.	Compound Name	LogP[30]	Activity	PHASE predicted activity	HOMO (eV)	LUMO (eV)
1	3,7-dinitrofluoranthene	4.44	5.09	1.84	-0.25	-0.12
2	1,3-dinitropyrene	4.44	5.04	3.97	-0.24	-0.13
3	2,7-dinitropyrene	4.44	4.58	3.23	-0.23	-0.12
4	1-hydroxy-3-nitropyrene	4.66	3.87	2.70	-0.21	-0.11
5	3-nitrofluoranthene	4.69	3.67	1.82	-0.24	-0.12
6	1,2,4-trinitrofluoranthene	4.18	3.56	1.60	-0.26	-0.14
7	4-nitropyrene	4.69	3.39	2.38	-0.22	-0.11
8	2,5-dinitrofluorene	3.71	3.20	1.68	-0.25	-0.12
9	2-bromo-7-nitrofluorene	4.83	3.06	0.96	-0.24	-0.10

10	2-nitroanthracene	4.23	2.95	2.57	-0.22	-0.11
11	2-(acetylamino)-7-nitrofluorene	3.08	2.85	3.08	-0.22	-0.10
12	2,8-dinitrophenazine	2.29	2.75	2.33	-0.26	-0.14
13	1-nitrofluoranthene	4.69	2.74	1.74	-0.24	-0.12
14	2-cyano-7-nitrofluorene	3.40	2.51	3.50	-0.25	-0.11
15	1-amino-8-nitropyrene	3.63	2.43	2.62	-0.19	-0.10
16	2-methyl-7-nitrofluorene	4.62	2.36	0.06	-0.23	-0.10
17	1,8-dinitro-9,10,11,12-tetrahydrobenzo[e]pyrene	6.01	2.19	2.61	-0.22	-0.13
18	2-nitro-9,10-dihydrophenanthrene	4.53	1.99	1.19	-0.24	-0.10
19	5-nitroacenaphthylene	3.36	1.91	0.40	-0.24	-0.12
20	6-nitrochrysene	5.41	1.75	1.79	-0.23	-0.11
21	2-hydroxy-7-nitrofluorene	3.43	1.68	1.46	-0.22	-0.10
22	2,4,3',4'-tetranitrobiphenyl	3.00	1.54	1.53	-0.28	-0.13

Table 1b:The actual and predicted mutagenicity values test set of compounds with their logP (taken from reference 30) and calculated salvation, LUMO energy at B3LYP/3-21G* level of theory.

S. No.	Compound Name	LogP[30]	Activity	PHASE predicted activity	HOMO (eV)	LUMO (eV)
23	8-hydroxy-1-nitropyrene	4.19	1.49	2.93	-0.21	-0.11
24	2-nitrocarbazole	3.51	1.01	0.24	-0.24	-0.12
25	6-nitroindene	2.74	0.96	-0.44	-0.24	-0.10
26	3-nitro-9,10,11,12-tetrahydrobenzo[e]pyrene	6.26	0.78	2.36	-0.22	-0.11
27	4-nitrostilbene	4.18	0.69	-1.08	-0.22	-0.11
28	5-nitro-1,10-phenanthroline	1.84	0.59	0.22	-0.26	-0.12
29	5-nitroindole	2.13	0.57	-0.82	-0.23	-0.09
30	2-nitrobenz[l]aceanthrylene	5.07	0.26	2.50	-0.23	-0.12
31	2-methyl-7-nitroindazole	1.77	0.23	-0.65	-0.23	-0.10
32	7-nitroindazole	1.75	0.11	-0.47	-0.25	-0.11
33	2-nitrobenzimidazole	1.59	0.00	-0.49	-0.25	-0.12
34	5-nitroindoline	2.07	-0.17	-0.80	-0.20	-0.08
35	2,4,2'-trinitrobiphenyl	3.26	-0.19	0.81	-0.27	-0.12
36	2-nitronaphthalene	3.24	-0.30	-0.50	-0.24	-0.10
37	8-nitro-2,3,7-trichlorodibenzo-1,4-dioxin	6.68	-0.53	0.44	-0.23	-0.11
38	1,3,6,8-tetranitronaphthalene	2.29	-0.70	0.59	-0.29	-0.14
39	1-methyl-5-nitroindazole	1.77	-0.82	0.39	-0.24	-0.10
40	6-nitroquinoline	1.84	-1.08	-0.29	-0.26	-0.11
41	3-chloro-4-fluoronitrobenzene	2.74	-1.21	-0.87	-0.28	-0.11
42	2-bromo-4,6-dinitroaniline	2.78	-1.32	-0.62	-0.24	-0.11
43	2,3-dichloronitrobenzene	3.05	-1.51	-0.44	-0.27	-0.11

Table 1b:The actual and predicted mutagenicity values test set of compounds with their logP (taken from reference 30) and calculated salvation, LUMO energy at B3LYP/3-21G* level of theory.

S. No.	Compound Name	LogP[30]	Activity	PHASE predicted activity	HOMO (eV)	LUMO (eV)
44	4-amino-3'-nitrobiphenyl	2.68	-1.52	-0.67	-0.19	-0.10
45	4-nitrobenzaldehyde	1.56	-1.64	-0.76	-0.27	-0.12
46	5-nitrobenzimidazole	1.64	-1.83	-1.11	-0.25	-0.10
47	2-nitrobenzaldehyde	1.74	-1.92	-1.60	-0.26	-0.12
48	4-chloro-2-nitroaniline	2.72	-2.00	-1.85	-0.22	-0.10
49	4-nitroanisole	2.03	-2.70	-1.66	-0.24	-0.10

Interpretation of QSAR model:

The major advantage of 3D-QSAR techniques like PHASE is the cubes generated using PLS regression, which could be visualized in 3D space with respect to various properties and can guide the various key determinants responsible for observed activity. Figure 2 shows cubes generated for hydrophobic, electron withdrawing and hydrogen bond donor properties using QSAR model. Most mutagenic ligand, 1,8-dinitropyrene is included for better visualization. In Figure 2a, green cubes represent the sterically favored spatial regions for mutagenicity, while magenta cubes represent the sterically disfavored regions for mutagenicity. Clear predominance of green cubes in the vicinity of fused pyrene moiety indicates that larger fused hydrophobic groups contribute positively towards mutagenicity. This observation is in accordance with literature reports where it was found that, planarity of the molecules plays a key role in forming stable mutagen-DNA, making them potential mutagens [45, 46]. The bulkier groups like phenyl, which may alter the planarity of the molecule, making the intercalation with DNA difficult may turn out to be less mutagenic. The QSAR models generated by Hansch et al. [1] also highlighted the importance of hydrophobic parameter, logP for mutagenicity.

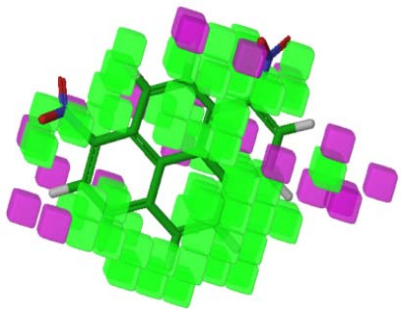

Fig. 2a: Pictorial representation of the contours generated for various properties, a) hydrophobic property; the green cubes indicate favorable regions while violet cube indicates unfavorable hydrophobic regions for the activity.

The model showed that, compounds with higher logP values are likely to be mutagenic [1]. Nonetheless, the logP does not give idea of three-dimensional arrangement, shape and size of hydrophobic groups, which appear to be critical in determining the mutagenicity of a molecule. For instance, the activity of a non-mutagenic compound, 1,2,3-trichloro-4-nitrobenzene, (actual log mutagenicity: -2.94) was highly overestimated (predicted log mutagenicity: 0.18) by the Hansch model [1], due to the high logP value 3.61, owing to presence of three chloro atom substitutions. On the other hand, the model generated here predicted reasonably low mutagenicity for this compound. Furthermore, the visualization of green cubes clearly predicts this compound as non-mutagenic. Thus, the three-dimensional representation of hydrophobic property has clear advantage over the simple logP for mutagenicity prediction.

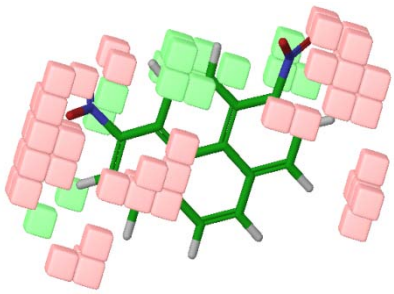

Fig. 2b: Electron withdrawing groups, the red cubes indicate favorable regions while light green cube indicates unfavorable region for the activity.

In Figure 2b, red color cubes represents electron withdrawing group favored regions for mutagenicity, while light green color cubes represents electron withdrawing group disfavored the regions for mutagenicity. The presence of more red cubes points the fact that nitroaromatic compounds with electron withdrawing group substitutions are likely to be more mutagenic. All most mutagenic compounds have two or more nitro group substitutions. Vance et al. [47] also noted the negative effect of electron donating substituents on the mutagenicity pointing out that p-dinitrobenzene is mutagenic while p-nitrophenol is not. In Figure 2c, orange cubes represent the hydrogen bond donor group regions disfavored for mutagenicity, while light blue cubes represents the hydrogen bond group donor favored regions for mutagenicity. Thus, substitution of hydrogen bond donor group in the vicinity of nitro group should decrease the mutagenicity. In this regard, 2-nitro-m-phenylenediamine with two hydrogen bond donor amino groups in the vicinity of nitrogroup was found to be non-mutagenic.

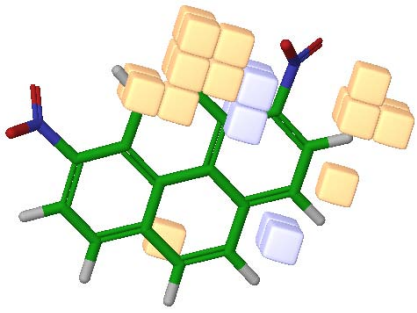

Fig. 2c: Hydrogen bond donor property; the blue cubes indicate favorable regions while orange cube indicates unfavorable region for the activity.

Thus, planar hydrophobic molecules with hydrogen bond acceptor and electron donating substitutions are likely to be mutagenic.

Density functional theory calculations:

All compounds were optimized at B3LYP/3-21G* level using PBF salvation model. The corresponding bond lengths (distances) and bond angles were in good agreement.

Molecular electrostatic potential (MESP) profiles:

The results show that most of the mutagenic nitroaromatic compounds share specific electronic properties and are different from non-mutagenic compounds. For comparative purpose, the MESP of eight most mutagenic compounds viz. 1,8-dinitropyrene, 3,7-dinitrofluoranthene, 1,6-dinitropyrene, 1,3-dinitropyrene, 3,9-dinitrofluoranthene, 1,3,6-trinitropyrene, 1,3,6,8-tetranitropyrene and 2,7-dinitropyrene; and eight non-mutagenic compounds viz. 2-nitro-m-phenylenediamine, 1,2,3-trichloro-4-nitrobenzene, 8-nitroquinalidine, 2-nitroanisole, 4-nitroanisole, 2-aminoanisole, 2-nitrophenetole and 3-amino-2'-nitrobiphenyl; are discussed here, but the trend of MESP remains similar for rest of compounds based on their mutagenicity value. MESP plotted onto constant electron density surface of 0.01 e/au^3 for all compounds showed the presence of localized most electronegative potential region (red color) near the oxygen atoms of the nitro group, the most mutagenic compounds have two or more localized most electronegative potential regions owing to presence of two to more nitro groups, while non-mutagenic compounds have only one localized most electronegative potential region in the vicinity of nitro group (Figure 3).

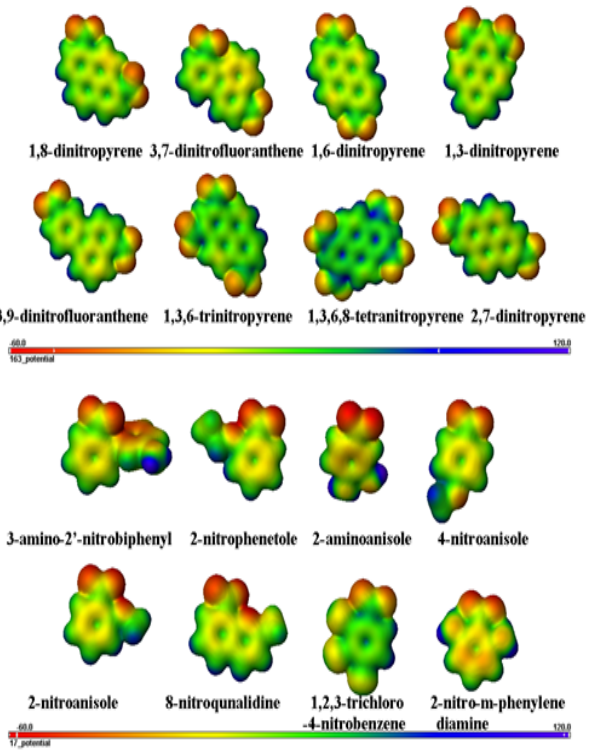

Fig. 3: MESP superimposed onto a surface of constant electron density (0.01 e/au^3) showing the most positive potential region (deepest blue color) and the most negative potential region (deepestred color). Each compound was color-coded using a range of MESP from -60 to 120 kcal/mol.

The 3D electrostatic potential profiles beyond the van der Waals surface of the molecules at -25.0 kcal/mol (Figure 4) clearly support this observation, where two or more distinct negative blue-shaped potential regions were visible in the vicinity of nitro group in most active compounds while only one negative potential region is present in the vicinity of nitro group.

This implies the direct correlation of more nitro groups in molecule to their mutagenicity potential. In few non-mutagenic compounds like 2-nitrophenetole, 2-nitroanisole, 8-nitroquinalidine, the localized negative potential of oxygen atoms of nitro group extends laterally over the oxygen or nitrogen atom of substitution in the vicinity. This observation is peculiar for non-mutagenic compounds, thus compound with an electronegative atom substitution in the vicinity of nitrogroup are likely to be nonmutagenic.

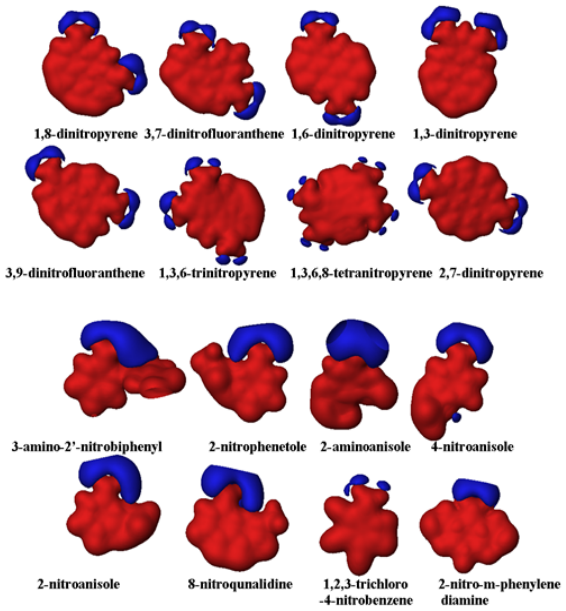

Fig. 4: Three-dimensional isopotential contours of MESP at -25 kcal/mol showing negative potential regions (blue colored counters) around the oxygen atoms of the nitro group.

Lowest unoccupied and highest occupied molecular orbitals (LUMOs and HOMOs)

The orbital energies of frontier orbitals, which are quantum chemical descriptors, were calculated for the whole dataset. Both the HOMO and LUMO energies are small, ranging between -0.29 to -0.17 and -0.15 to -0.08 eV respectively, indicating the fragile nature of bound electrons (Table 1a-b). Due to small values of HOMO and LUMO, both rapid electron transfer and exchange are equally possible, making these molecules very reactive. In particular, a small HOMO and LUMO gap signifies less stability. Such molecules are likely to undergo changes in the charge distribution through rapid electron transfer between HOMO and LUMO. Mechanistically LUMO plays important role than the HOMO. LUMO sites are scattered over the nitro group and to small extent over the aromatic ring plane, implying the nucleophilic susceptibility of this part of molecule (Figure 5).

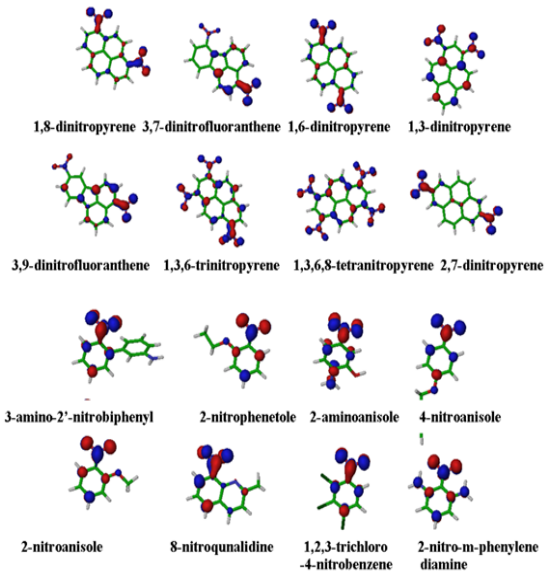

Fig. 5: Distribution of LUMO energies for some of the mutagenic and non-mutagenic compounds.

CONCLUSION

An atom based QSTR model was generated for prediction of mutagenicity of the compounds. The visualization of different properties highlighted several important points such as the molecules with more fused planar hydrophobic rings having hydrogen bond acceptor and electron donating substitutions are likely to be mutagenic. Specific calculated quantum chemical properties provide additional mechanistic details about the mutagenicity of these compounds. This study shows that most of the mutagenic compounds have two or more negative potential regions owing to presence of more than one nitro group. Also, the aromatic ring plane in case of highly mutagenic compounds is less electronegative compared to non-mutagenic compounds. Specific electronic properties such as HOMO and LUMO indicate that the molecules are very reactive in nature. Moreover, the LUMO energies calculated at higher level of theory can be used to refine existing models. The findings of this study would be useful to understand the mutagenicity of nitroaromatic compounds and to design non-mutagenic compounds.

ACKNOWLEDGEMENTS

Nilesh Tawari is thankful to Department of Biotechnology, New Delhi, Arundhati Lele is thankful to Council of Scientific and Industrial Research, New Delhi and Mihir Khambete is thankful to Department of Science and Technology, New Delhi, for financial support.

REFERENCES

1. Debnath AK, Lopez de Compadre RL, DebnathG, Shusterman AJ, Hansch C. Structure-activity relationship of mutagenic aromatic and heteroaromatic nitro compounds. Correlation with molecular orbital energies and hydrophobicity. J Med Chem 1991;34:786-97.
2. Boelsterli UA, Ho HK, Zhou S, Leow KY. Bioactivation and hepatotoxicity of nitroaromatic drugs. J Curr Drug Metab 2006;7:715-27.
3. Matsumoto M, Hashizume H, Tomishige T, Kawasaki M, Tsubouchi H, Sasaki H *et al*. OPC-67683, a nitro-dihydroimidazooxazole derivative with promising action against tuberculosis *in vitro* and in mice. J PLoS Med 2006;3:2131-44.
4. Stover CK, Warrener P, VanDevanter DR, Sherman DR, Arain TM, Langhorne MH *et al*. A small-molecule nitroimidazopyran drug candidate for the treatment of tuberculosis. J Nature 2000;405:962-6.
5. Tyagi S, Nuermberger E, Yoshimatsu T, Williams K, Rosenthal I, Lounis N *et al*. Bactericidal activity of the nitroimidazopyran PA-824 in a murine model of tuberculosis. J Antimicrob Agents Chemother 2005;49:2289-93.
6. Purohit V, Basu A K. Mutagenicity of nitroaromatic compounds. J Chem Res Toxicol 2000;13:673-92.
7. Sabbioni G. Hemoglobin binding of nitroarenes and quantitative structure activity relationships. J Chem Res Toxicol 1994;7:267-74.
8. Mc Cann J, Choi E, Yamasaki E, Ames BN. Detection of carcinogens as mutagens in the Salmonella/microsome test:assay of 300 chemicals. L Proc Natl Acad Sci USA 1975;72:5135-9.
9. Mc Cann J, Spingarn NE, Kobori J, Ames BN. Detection of carcinogens as mutagens:bacterial tester strains with R factor plasmids. J Proc Natl Acad Sci USA 1975;72:979-83.
10. Zeiger E. Carcinogenicity of mutagens:predictive capability of the Salmonella mutagenesis assay for rodent carcinogenicity. J Cancer Res 1987;47:1287-96.
11. Benigni R, Bossa C. Mechanisms of Chemical Carcinogenicity and Mutagenicity:A Review with Implications for Predictive Toxicology. J Chem Rev 2011;111:2507-36.
12. Isayev O, Rasulev B, Gorb L, Leszczynski J. Structure-toxicity relationships of nitroaromatic compounds. Mol Divers 2006;10:233-45.
13. Basak SC, Mills DR, Balaban AT, Gute BD. Prediction of mutagenicity of aromatic and heteroaromatic amines from

Structure:A hierarchical QSAR approach. J ChemInf Comput Sci 2001;41:671-8.
14. Benigni R, Giuliani A, Franke R, Gruska A. Quantitative structure-activity relationships of mutagenic and carcinogenic aromatic amines. J Chem Rev 2000;100:3697-714.
15. Benigni R, Zito R. Designing safer drugs:(Q)SAR-based identification of mutagens and carcinogens. J Curr Top Med Chem 2003;3:1289-300.
16. Gramatica P, Consonni V, Pavan M. Prediction of aromatic amines mutagenicity from theoretical molecular descriptors. J SAR QSAR Environ Res 2003;14:237-50.
17. Richard AM. International Commission for Protection Against Environmental Mutagens and Carcinogens. Application of SAR methods to non-congeneric data bases associated with carcinogenicity and mutagenicity: issues and approaches. J Mutat Res 1994;305:73-97.
18. Ashby J, Tennant RW. Chemical structure, Salmonella mutagenicity and extent of carcinogenicity as indicators of genotoxic carcinogenesis among 222 chemicals tested in rodents by the U.S. NCI/NTP. J Mutat Res 1988;204:17-115.
19. Hoel DG, Haseman JK, Hogan MD, Huff J, McConnell EE. The impact of toxicity on carcinogenicity studies: implications for risk assessment. J Carcinogenesis 1988;9:2045-52.
20. Mortelmans K, Zeiger E. The Ames Salmonella/microsome mutagenicity assay. J Mutat Res 2000;455:29-60.
21. Shelby MD. The genetic toxicity of human carcinogens and its implications. J Mutat Res 1988;204:3-15.
22. Benigni R. Structure-activity relationship studies of chemical mutagens and carcinogens:mechanistic investigations and prediction approaches. J Chem Rev 2005;105:1767-800.
23. Maynard AT, Pedersen LG, Posner HS, McKinney JD. An Ab initio study of the relationship between nitroarene mutagenicity and electron affinity. J Mol Pharmacol 1986;29:629-36.
24. Hu J, Wang W, Zhu Z, Chang H, Pan F, Lin B. Quantitative Structure–Activity Relationship Model for Prediction of Genotoxic Potential for Quinolone Antibacterials. J Environ Sci Technol 2007;41:4806-12.
25. Smith C. QSAR treatment of multiple toxicities:the mutagenicity and cytotoxicity of quinolines. J Mutat Res 1997;379:167-75.
26. Tang Y, Chen K, Jiang H, Ji R. QSAR/QSTR of fluoroquinolones:an example of simultaneous analysis of multiple biological activities using neural network method. J Eur Jrnl Med Chem 1998;33:647-58.
27. Nair PC, Sobhia ME. Comparative QSTR studies for predicting mutagenicity of nitro compounds. J Mol Graph Model 2008;26:916-34.
28. Bhat KL, Hayik S, Sztandera L, Bock CW. Mutagenicity of Aromatic and Heteroaromatic Amines and Related Compounds:A QSAR Investigation. J QSAR and Comb Sci 2005;24:831-43.
29. Hatch FT, Colvin ME. Quantitative structure–activity (QSAR) relationships of mutagenic aromatic and heterocyclic amines. J Mutat Res 1997;376:87-96.
30. Tchounwou PB, Wilson B, Ishaque A, Ransome R, Huang M-J, Leszczynski J. Toxicity Assessment of Atrazine and Related Triazine Compounds in the Microtox Assay, and Computational Modeling for Their Structure-Activity Relationship. Int J Mol Sci 2000;1:63-74.
31. Bruce E, Autenrieth R, Burghardt R, Donnelly KC, McDonald T. Using Quantitative Structure-Activity Relationships (QSAR) to Predict Toxic Endpoints for Polycyclic Aromatic Hydrocarbons (PAH). J Toxicol Environ Health A 2008;71:1073-84.
32. Papa E, Pilutti P, Gramatica P. Prediction of PAH mutagenicity in human cells by QSAR classification. J SAR and QSAR Environ Res 2008;19:115-27.
33. Schmidt TJ, Heilmann J. Quantitative Structure-Cytotoxicity Relationships of Sesquiterpene Lactones derived from partial charge (Q)-based fractional Accessible Surface Area Descriptors (Q_frASAs). J Quant Struct Act Relat 2002;21:276-87.
34. Scotti MT, Fernandes MB, Ferreira MJP, Emerenciano VP. Quantitative structure–activity relationship of sesquiterpene lactones with cytotoxic activity. J Bioorg Med Chem 2007;15:2927-34.
35. Goldring JM, Ball LM, Sangaiah R, Gold A. Mutagenic activity of nitro-substituted cyclopenta-fused polycyclic aromatic hydrocarbons towards Salmonella typhimurium. J Mutat Res 1987;187:67-77.
36. Rosenkranz HS, Mermelstein R. Mutagenicity and genotoxicity of nitroarenes. All nitro-containing chemicals were not created equal. J Mutat Res 1983;114:217-67.
37. Zielinska B, Arey J, Harger WP, Lee RW. Mutagenic activities of selected nitrofluoranthene derivatives in *Salmonella typhimurium* strains TA98, TA98NR and TA98/1,8-DNP6. J Mutat Res 1988;206:131-40.
38. Dixon SL, Smondyrev AM, Knoll EH, Rao SN, Shaw DE, Friesner RA. PHASE: A new engine for pharmacophore perception, 3D QSAR model development, and 3D database screening:1. Methodology and preliminary results. J Comput Aided Mol Des 2006;20:647-71.
39. Becke AD. Density-functional thermochemistry III. The role of exact exchange. J Chem Phys 1993;98:5648-52.
40. Becke AD. A new mixing of Hartree–Fock and local density-functional theories. J Chem Phys 1993b;98:1372-77.
41. Lee C, Yang W, Parr RG. Development of the Colle-Salvetti correlation-energy formula into a functional of the electron density. J Phys Rev B Condens Matter 1988;37:785-9.
42. Binkley JS, Pople JA, Hehre WJ. Self-consistent molecular orbital methods. 21. Small split-valence basis sets for first-row elements. J Am Chem Soc 1980;102:939-47.
43. Gordon MS, Binkley JS, Pople JA, Pietro WJ, Hehre WJ. Self-consistent molecular-orbital methods. 22. Small split-valence basis sets for second-row elements. J Am Chem Soc 1982;104:2797-803.
44. Pietro WJ, Francl MM, Hehre WJ, DeFrees DJ, Pople JA, Binkley JS. Self-consistent molecular orbital methods. 24. Supplemented small split-valence basis sets for second-row elements. J Am Chem Soc 1982;104:5039-48.
45. Glende C, Klein M, Schmitt H, Erdinger L, Boche G. Transformation of mutagenic aromatic amines into non-mutagenic species by alkyl substituents. Part II: Alkylation far away from the amino function. J Mutat Res 2002;515:15-38.
46. Klein M, Voigtmann U, Haack T, Erdinger L, Boche G. From mutagenic to non-mutagenic nitroarenes: Affect of bulky alkyl substituents on the mutagenic activity of 4-nitrobiphenyl in *Salmonella typhimurium*. Part I. Substituents ortho to the nitro group and in 2'-position. J Mutat Res 2000;467:55-68.
47. Vance WA, Levin DE. Structural features of nitroaromatics that determine mutagenic activity in *Salmonella typhimurium*. J Environ Mutagen 1984;6:797-811.